CrystEngComm

Accepted Manuscript

ROYAL SOCIETY OF CHEMISTRY

www.rsc.org/crystengcomm

CrystEngComm

RSCPublishing

ARTICLE

Guest Dependent Dielectric Properties of Nickel(II)-Based Supramolecular Networks

Cite this: DOI: 10.1039/xoxxoooooox

Shruti Mendiratta,[a,b,c] Muhammad Usman,[a] Tzuoo-Tsair Luo,[a] Shang-Fan Lee,[d] Ying-Chih Lin*[b] and Kuang-Lieh Lu*[a]

Received ooth January 2012,
Accepted ooth January 2012

DOI: 10.1039/xoxxoooooox

www.rsc.org/

Two Nickel(II)-based low dielectric supramolecular compounds $\{[Ni_2(bbim)(H_2bbim)_4]\cdot 2CH_3COO\cdot CH_3CN\}_2$ (**1**, H_2bbim = bisbenzimidazole) and (±)-$[Ni(H_2bbim)_3]\cdot 2Cl\cdot 2H_2O$ (**2**) were synthesized and characterized by single-crystal X-ray crystallography. Compound **1** was found to have a dimeric structure with guest molecules such as acetate ions and acetonitrile in its environment, while compound **2** had a monomeric structure with chloride ions and water molecules associated with it. Both compounds are highly thermally stable, especially compound **1**, which is stable at temperatures of up to 500 °C. More importantly, compound **1** adopts a sharp different frequency dependent dielectric behaviour when compared with **2**. Compound **2** with highly polarizable guest molecules showed a significant higher value of dielectric constant ($\varepsilon'_r(\omega)$ = 12.6 at 40 Hz) than that of **1** ($\varepsilon'_r(\omega)$ = 4.76 at 40 Hz), indicating that solvent molecules and counterions play a crucial role in regulating the value of the dielectric constant. This study serves as a good example of the design of both high and low-κ materials with a judicious selection of guest molecules in the supramolecular networks.

1. Introduction

Self-assembly processes involving metal ions and well-designed organic ligands give rise to interesting functional hybrid materials. Recently, supramolecular networks and coordination polymers have found wide applications due to their versatile properties such as their ability to function as molecular sensors,[1-5] molecular switches,[6-9] catalysis,[10-13] self-healing polymers,[14-17] synthetic ion channels[18-21] and in the treatment of radioactive waste.[22,23] However, reports concerning the dielectric properties of these materials are sparse even though they possess advantageous properties of functioning as both inorganic and organic compounds.[24-30] The dielectric properties of hybrid materials are of immense importance as the field of solid state electronics continues to expand rapidly. Dielectric materials find applications in high technology fields such as filters, capacitors, resonators, solid-state transducers and other key components in microelectronic systems.[31-35] Low-κ materials, in particular, are able to decrease cross-talk noise, propagation delay and power dissipation when incorporated in device systems, therefore the search for new low-κ dielectric materials have gained increased recognition.[36] One of the criteria used for selecting a suitable low-κ dielectric material is the absence of electrical order or dielectric anomalies which are a result of order-disorder processes of polar and H-bonded guest molecules that are present in the void spaces of host structures. Such a behaviour has recently been reported by Sánchez-Andújar *et. al.*[37] in the case of the hybrid compound Co_2(1,4-bdc)$_2$(dabco)·[4DMF·H_2O], which shows a colossal dielectric constant at room temperature ($\varepsilon'_r \approx 5000$ at 300 K for υ = 100 Hz). Experimental results have shown that, a slight modification in reactants, periodic atom arrangements and density levels along the crystal lattice direction can result in different dielectric properties.[38,39]

As part of our ongoing efforts in the design and synthesis of functional crystalline materials,[40-46] we report herein on the frequency dependent dielectric behaviour of two intriguing nickel(II)-based supramolecular compounds $\{[Ni_2(bbim)(H_2bbim)_4]\cdot 2CH_3COO\cdot CH_3CN\}_2$ (**1**) (H_2bbim = bisbenzimidazole) and (±)-$[Ni(H_2bbim)_3]\cdot 2Cl\cdot 2H_2O$ (**2**). Importantly, compounds **1** and **2** feature 1) preparation through a one-step self-assembly process in high yields; 2) large cavities that can accommodate guest molecules and counterions of varying polarity; 3) unique acetate dimers displaying rare C–H···O hydrogen bonding encapsulated in the network of **1**; 4) specific anion-solvent pair imparted dramatically different dielectric properties to both compounds. In particular, a significant reduction in the value of the dielectric constant ($\varepsilon'_r(\omega)$) was observed when highly polarizable guest molecules in compound **2** were replaced by less polarizable ones in compound **1**. In comparison to SiO_2 ($\varepsilon'_r(\omega)$ = 3.91), compound **1** was found to be a good low-κ material ($\varepsilon'_r(\omega)$ = 3.03 at 10 kHz) in the high frequency region. To the best of our

knowledge, such supramolecular networks with specific anion-solvent pair and guest dependent dielectric properties have not yet been realized.

2. Experimental Section

2.1 General Information

All chemicals were purchased commercially and used as received without further purification. Elemental analyses were conducted on a Perkin-Elmer 2400 CHN elemental analyzer. Infrared spectra were recorded in the range of 4000–400 cm^{-1} on a Perkin-Elmer Paragon 1000 FT-IR spectrophotometer. Thermogravimetric analysis (TGA) was performed under nitrogen with a Perkin-Elmer TGA-7 TG analyzer. Powder X-ray diffraction (PXRD) data were recorded on a Phillips X'Pert Pro diffractometer operated at a voltage of 40 kV and a current of 30 mA with Cu-Kα radiation (λ = 1.5406 Å).

2.2 Synthesis of $\{[Ni_2(bbim)(H_2bbim)_4]\cdot 2CH_3COO\cdot CH_3CN\}_2$ (1)

Compound $\{[Ni_2(bbim)(H_2bbim)_4]\cdot 2CH_3COO\cdot CH_3CN\}_2$ (**1**) was synthesized through a self-assembly process by reacting $NiCl_2.6H_2O$ (71.3 mg, 0.30 mmol), H_2bbim (35.1 mg, 0.15 mmol) and malic acid (20.1 mg, 0.15 mmol) in a CH_3CN/H_2O (4 mL:2 mL) solution containing 0.5 mL of 1 M KOH solution under hydrothermal conditions at 180 °C for 72 h followed by allowing the solution to slowly cool at a rate of –2.08 °C/h. Dark green crystals of **1**, suitable for single-crystal X-ray diffraction studies were obtained by filtration and washing with deionized water and acetone, followed by air-drying. Yield: 52.6% (22.9 mg, 0.0079 mmol) based on H_2bbim. Anal. Calcd (%) for $C_{152}H_{114}N_{42}Ni_4O_8$: C, 63.13; H, 3.97; N, 20.34. Found: C, 63.02; H, 3.80; N, 20.08. IR (KBr/pellet, cm^{-1}): ν = 3070 (vw), 1590 (s), 1556 (s), 1498 (w), 1463 (w), 1420 (vs), 1349 (s), 1314 (m), 1269 (w), 1258 (s), 1227 (w), 1142 (m), 1117 (w), 1026 (m), 994 (m), 894 (w), 826 (w), 779 (s), 741 (vs), 648 (m), 603 (m), 584 (w), 539 (w) cm^{-1}.

2.3 Synthesis of (±)-$[Ni(H_2bbim)_3]\cdot 2Cl\cdot 2H_2O$ (2)

Compound (±)-$[Ni(H_2bbim)_3]\cdot 2Cl\cdot 2H_2O$ (**2**) was prepared by reacting $NiCl_2.6H_2O$ (285.1 mg, 1.2 mmol) and H_2bbim (140.6 mg, 0.6 mmol) in a $MeOH/H_2O$ (10 mL, 1:1) solution under hydrothermal conditions at 160 °C for 72 h followed by allowing the solution to slowly cool at a rate of –2.08 °C/h. Pale green crystals were separated by filtration, washed with deionized water and acetone, then dried in air. Yield: 87.5% (152 mg, 0.175 mmol) based on H_2bbim. Anal. Calcd (%) for $C_{42}H_{34}Cl_2N_{12}NiO_2$: C, 58.09; H, 3.94; N, 19.35. Found: C, 58.32; H, 3.93; N, 19.40. IR (KBr/pellet, cm^{-1}): ν = 3392 (w), 3065 (s), 1586 (s), 1501 (w), 1449 (w), 1419 (vs), 1384 (w), 1348 (s), 1323 (w), 1268 (m), 1231 (w), 1187 (w), 1146 (m), 1114 (vw), 1032 (s), 998 (s), 934 (w), 896 (m), 852 (vw), 829 (m), 737 (vs), 662 (w), 627 (vw), 605 (m), 586 (m) cm^{-1}.

2.4 Single crystal X-ray crystallographic analyses

Single-crystal X-ray diffraction for compounds **1** and **2** was performed by using a Bruker-Nonius Kappa CCD diffractometer with graphite-monochromated Mo Kα radiation. Data collection parameters of compounds **1** and **2** are listed in Table 1 as well as Table S1 and S2 (See Supplementary Information). The structures were solved using direct methods and refined using the SHELXS-97 program[47] by full-matrix least squares on F^2 values for **1** and **2**. In addition to SHELX-97 program, the structural data were refined using WINGX[48] in case of compound **2**. All non-hydrogen atoms were refined anisotropically, whereas the hydrogen atoms were placed in ideal, calculated positions, with isotropic thermal parameters riding on their respective carbon atoms.

2.5 Dielectric Characterization Techniques

Complex dielectric properties of powder samples were measured using an Agilent 4294A impedance analyzer connected to an Agilent 16451B dielectric test fixture over a frequency range of 40 Hz to 10 kHz at room temperature. Pellets of compounds **1** and **2** were prepared from powder samples through high pressure (40 MPa). A contact electrode method was used with 5 mm guarded/unguarded electrodes. The capacitance (Cp) and dielectric loss (D) were directly recorded from the impedance analyzer. The dielectric constant was determined by equation 1:

$$k = Cpd/\varepsilon_0 A \qquad (1)$$

Here, ε_0 is the dielectric permittivity in a vacuum (8.85×10^{12} F/m); A is the area of the electrode (m^2), and d is the thickness of the film (m).

3. Results and Discussion

3.1 Synthesis

Bisbenzimidazole compounds belong to a special class of ligands for the construction of novel coordination polymers, as they can participate in mono-, bi-, multidentate and chelating coordination modes with central metal ions. Herein, as shown in Scheme 1, the reaction of $NiCl_2\cdot 6H_2O$ with the H_2bbim ligand under hydrothermal conditions resulted in the formation

Scheme 1 The synthesis of compounds **1** and **2**.

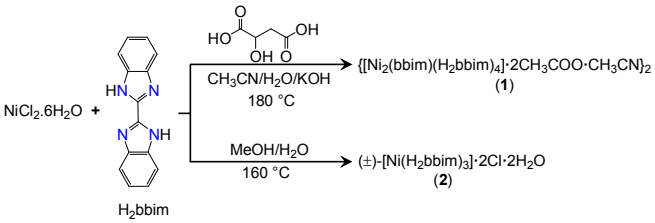

Table 1 Crystal data and structural refinement summary for complexes **1** and **2**

Complex	**1**	**2**
Empirical formula	$C_{152}H_{114}Ni_4N_{42}O_8$	$C_{42}H_{34}NiCl_2N_{12}O_2$
M	2891.69	868.42
Crystal system	Monoclinic	Orthorhombic
Space Group	$P2_1/c$	*Pnab*
a/Å	12.688(11)	12.256(2)
b/Å	37.728(3)	15.712(3)
c/Å	29.351(3)	20.787(4)
α (°)	90.00	90.00
β (°)	90.03	90.00
γ (°)	90.00	90.00
V/Å^3	14050(2)	4003.25(13)
Z	4	4
D_{calc}/g cm^{-3}	1.367	1.441
F(000)	5984	1792
μ/mm^{-1}	0.603	0.672
No. of unique reflcns	24743	3537
Reflcns used [$I > 2\sigma(I)$]	14610	2936
Goodness-of-fit on F^2	1.037	1.134
Final R indices [$I > 2\sigma(I)$][a]	R1 = 0.0752	R1 = 0.0422
	wR_2 = 0.1759	wR_2 = 0.1205

[a] $R1 = \Sigma||F_o| - |F_c||/\Sigma|F_o|$; $wR_2 = \Sigma[w(F_o^2 - F_c^2)^2]/\Sigma[w(F_o^2)^2]^{1/2}$.

of two supramolecular compounds $\{[Ni_2(bbim)(H_2bbim)_4]\cdot 2CH_3COO\cdot CH_3CN\}_2$ (**1**) and (±)-$[Ni(H_2bbim)_3]\cdot 2Cl\cdot 2H_2O$ (**2**). Even though the L-malic acid ligand was not involved in the formula, it acted as a template in the formation of **1**. We examined several routes to the synthesis of compound **1** in the absence of L-malic acid, but none was successful.

Compounds **1** and **2** were characterized by satisfactory elemental analyses, IR and X-ray diffraction analysis. FTIR patterns for both compounds are shown in Fig. S1 (ESI) and the crystal data are shown in Table 1 as well as Tables S1–S2 (ESI). Possible coordination modes of H_2bbim ligand are shown in Scheme S1 (ESI), and further structural details are described below.

3.2 Crystal Structure

$[Ni_2(bbim)(H_2bbim)_4]\cdot 2CH_3COO\cdot CH_3CN$ (1)

A single-crystal X-ray diffraction analysis showed that compound **1** crystallized in the monoclinic $P2_1/c$ space group. It has four crystallographically independent Ni(II) atoms and features a dimeric structure (Fig. 1a) with each pair of adjacent Ni(II) atoms bridged by the $bbim^{2-}$ ligand in a bis-bidentate fashion (Scheme S1, mode E, ESI) and the coordination sphere is completed with the chelating H_2bbim ligands (Scheme S1, mode A, ESI).

The Ni1 (or Ni2, Ni3, Ni4)) atom is six-coordinated by two nitrogen atoms from one bis-bidentate bbim ligand (Ni1–N1 2.115, Ni1–N2 2.135, Ni2–N3 2.153, Ni2–N4 2.089 Å) and four nitrogen atoms from two chelating H_2bbim ligands (Ni1–N5 2.113, Ni1–N6 2.110, Ni1–N9 2.169, Ni1–N10 2.102 Å), leading to a distorted octahedral coordination geometry. N1, N2, N6 and N9 comprise the equatorial plane, while the apical positions are occupied by N5 and N10 (N5–Ni1–N10 173.12°). Ni2 atoms are arranged in a similar fashion as that for the Ni1 atoms. The bite angle of Ni1–bbim (82.3°) is slightly larger than that of Ni1–H_2bbim (78.5–78.6°). As shown in Fig. 1a, the bis-bidentate ligand $bbim^{2-}$ locates on a symmetry center and bridges the two $Ni(H_2bbim)_2$ moieties to form a binuclear coordination cation with a Ni···Ni distance of 5.48 Å (between Ni1 and Ni2) and a distance of 5.5 Å between Ni3 and Ni4.

The four coordinated H_2bbim ligands are arrayed on the periphery of the binuclear unit as the second sphere receptors for anions via hydrogen bonding (Fig. 1a). Indeed, each binuclear cation is hydrogen bonded to four acetate anions with distances of N···O = 2.614(151)–2.822(59) Å (including Ni1, Ni2, N3 and Ni4) and angles of N–H···O = 149–174°. In addition, weak hydrogen bonding occurs between the nitrogen atom of CH_3CN and C–H bonds of acetate ion and bisbenzimidazole ligand (Fig. S2, ESI). The dimeric units are connected to each other via hydrogen bonding to give a 2D layer network on the *bc* plane (Fig. 1b). Interestingly, in this 2D network, the encapsulated acetate ions form cyclic dimers through C–H···O hydrogen bonding (Fig. 1c) which is a very rare case compared with the usual O–H···O bonding mode in carboxylic acid dimers.[49]

(±)-$[Ni(H_2bbim)_3]\cdot 2Cl\cdot 2H_2O$ (2)

In order to understand the difference in properties of compounds **1** and **2**, it is important to have a fundamental understanding of the crystal structure of compound **2**. In this case, compound **2** was found to be a racemic complex

crystallizing in the orthorhombic, *Pnab* space group. Here, each Ni (II) center is coordinated by six nitrogen atoms from three H_2bbim [Ni–N = 2.076–2.149 Å] in a chelating manner to give

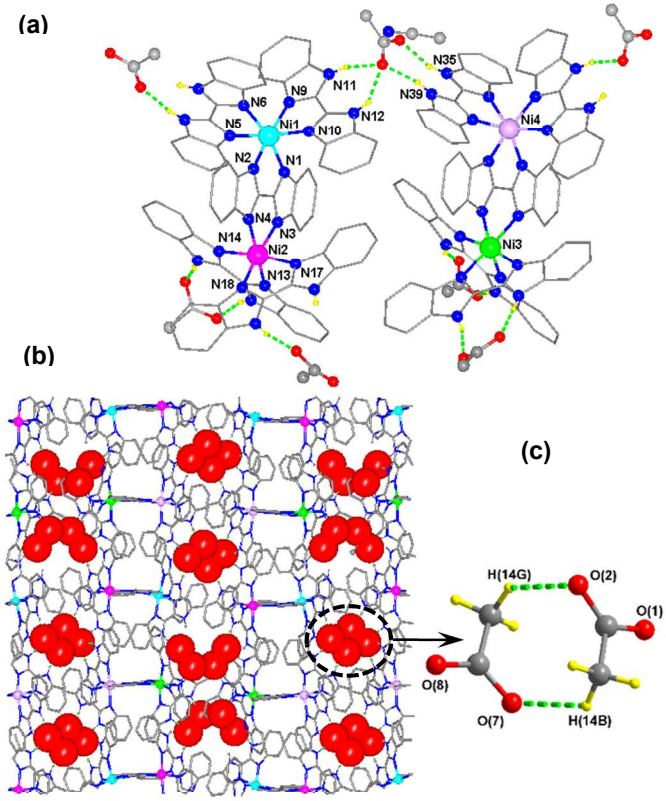

Fig. 1 (a) View of the coordination environment of Ni(II) ion in **1** displaying hydrogen bonding with CH_3COO^-, (b) 2D hydrogen-bonded net on the *bc* plane in **1**, (c) encapsulated acetate dimer showing the unusual C–H···O hydrogen bonding interactions.

a distorted octahedral geometry (Fig. 2a). It is noteworthy that, each Ni(II) cation is a chiral center showing either + or – non-superimposable mirror images, however the overall structure remains achiral. In contrast to the limited noncovalent interactions present in compound **1**, compound **2** was found to self-assemble through a wide variety of N–H···X, N–H···O, O–H···X, hydrogen bonds and π···π stacking as well as X···π (imidazolyl) charge-assisted interactions. Each $[Ni(H_2bbim)_3]^{2+}$ cation is hydrogen bonded to two chloride anions which are located at a distance of 3.110–3.172 Å and the angles of N–H···Cl = 153–161°C, and two water molecules with the distances of N···O = 2.731 Å and the angles of N–H···O = 158° as a smallest building unit. This compound possesses extensive hydrogen bonding, which arises from the monomeric unit and repeats itself throughout the crystal. Along the *ab* plane, four types of hydrogen bonds (Fig. 2b) are observed, the first of which can be observed between the Cl(1) atoms (green) and one of the N–H groups of the H_2bbim ligand (green dotted line), the second exists between Cl(2) (pink) and both the N–H groups of the H_2bbim ligand (purple dotted line), the third exists between electronegative oxygen atoms of water and one of the the N–H groups of two H_2bbim ligands (blue dotted line) and last one occurs between hydrogen atoms of water molecules and Cl(1) or Cl(2) (red dotted line).

Apart from hydrogen bonding in the structure, Cl···π interactions as well as π···π interactions can be observed which aid in arranging the monomeric units in a zipper like fashion. As proposed by Zhong *et. al.*, coordination of a positively charged metal ion greatly enhances the electron-deficient character of the imidazolyl ring and provides sufficient polarization to produce anion–π charge assisted interactions.[50] Cl···π

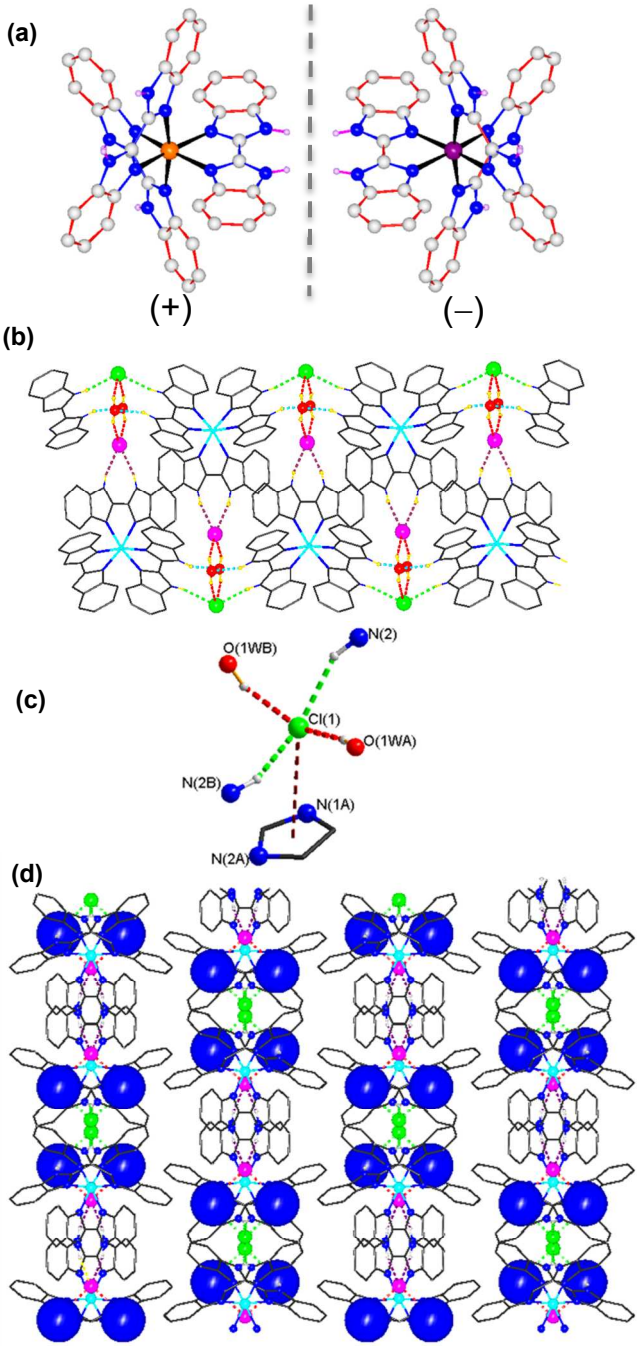

Fig. 2 (a) View of the coordination environment of Ni(II) ion in **2**, (b) 2D hydrogen-bonded net on the *ab* plane in **2**, showing four types of hydrogen bonds, (c) Cl···π interactions, (d) View of **2** along the *bc* plane showing space filling model of individual water molecules (blue).

interactions occur between the Cl(1) and the nearest imidazole unit (N–imidazole = 3.47 Å) of bisbenzimidazole ligand (Fig. 2c). Figure 2d shows the view along the *bc* plane. The position of water molecules (shown in blue) can be observed and the pattern is completely different in comparison to that for compound **1**.

3.3 Thermogravimetric Analysis

To assess the thermal stability and its structural variation as a function of the temperature, TGA analyses of the samples were performed. During the heating process, the TGA (Fig. 3) data indicated that compound **1** underwent a three step weight loss. There is a gradual loss of CH_3CN molecules up to a temperature of 244 °C and the acetate ions then slowly begin to decompose until the entire structure collapses at a temperature of 500 °C (Fig. S3, ESI). While in compound **2**, after the loss of guest water molecules, the structure is maintained until the temperature reaches 315 °C. The PXRD measurements (Fig. S4, ESI) confirm that the samples were pure.

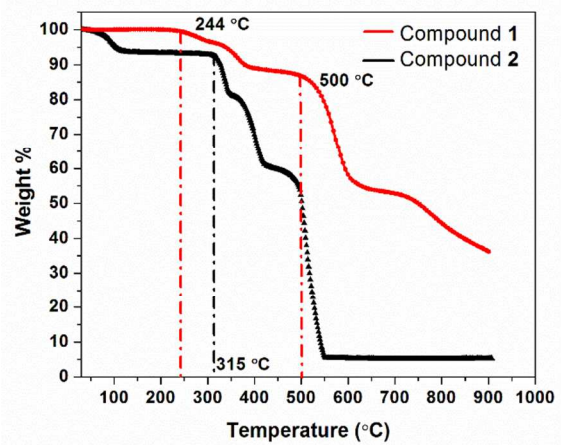

Fig. 3 Thermogravimetric curves of **1** and **2**.

3.3 Dielectric Properties

The dielectric properties of **1** and **2** were also investigated. Frequency dependent permittivity $[\varepsilon'_r(\omega) + \varepsilon''_r(\omega)]$ was measured from 40 Hz–10 kHz, where $\varepsilon'_r(\omega)$ is the dielectric constant and $\varepsilon''_r(\omega)$ is the dielectric loss. The former corresponds to the real part of the permittivity while the latter corresponds to the imaginary part. The dielectric constant in the range of 1–10 kHz is typically used to compare different low-κ dielectric materials for their use in microelectronics.[27] Our measurements indicated that the relative permittivity ($\varepsilon'_r(\omega)$) reached its highest value of 12.6 for compound **2** and a value of 4.76 for compound **1** at a very low frequency (Fig. 4a) and then rapidly decreased to 5.36 for compound **2** and 3.03 for compound **1** at 10 kHz, respectively.

The dielectric constant (κ) of a material is a complex function which depends on the density and total polarizability of its molecules.[51,52] Various factors contribute to the polarizability of molecules such as: space-charge polarization, dipolar interactions, atomic, ionic, distortions and electronic interactions. Compounds **1** and **2** contain the same metal center and ligand. No doubt, structural aspects like monomer and dimer cause the difference in the κ values, but more significant is the contribution of guest molecules. In compound **2**, extensive hydrogen bonding between free chlorides, the N–H group of imidazoles and free water molecules can transfer polarization between layers and encompasses the complete structure. The effect of guest molecules was also explained effectively by Cheetham and coworkers in the case of dense metal–organic frameworks (MOFs) with perovskite structures, for example, in alkylammonium transition metal formates such as $[(CH_3)_2NH_2][M(HCOO)_3]$ (M^{2+} = Zn^{2+}, Mn^{2+}, Co^{2+}, Fe^{2+} and Ni^{2+}).[53,54] Cooperative ordering by the dimethylamine (DMA) cations was found to be the reason for the formation of a polar structure and an extraordinary dielectric transition. Such polarization transfer cannot be observed in compound **1**, since hydrogen bonding is localized between the 2D layers. In particular, the hydrogen bonding between acetate dimers remains localized and does not spread out throughout the complete structure.

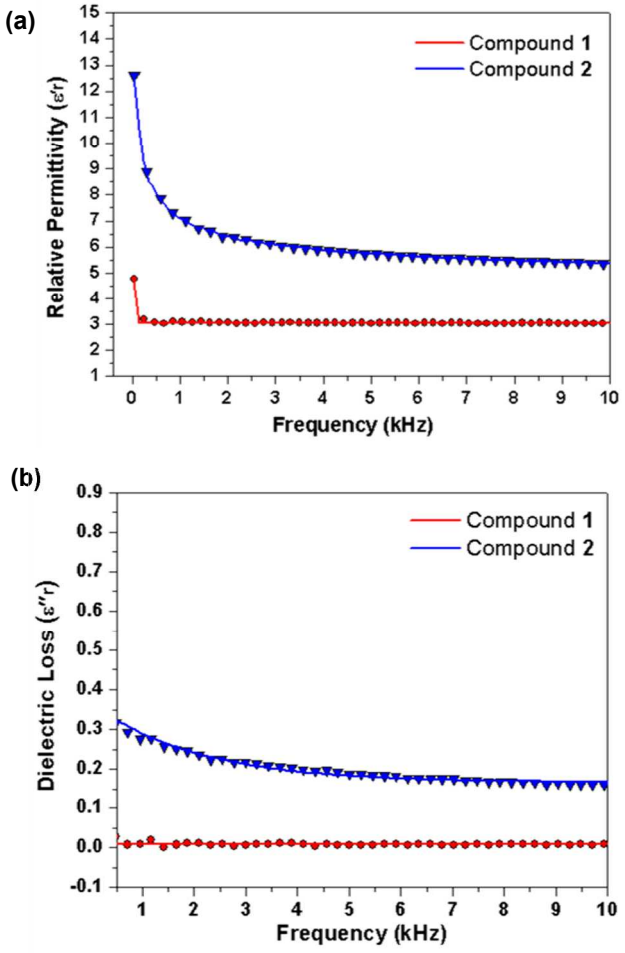

Fig. 4 (a) Variation of dielectric constants in **1** and **2** with change in frequency, (b) The corresponding variation of dielectric loss with change in frequency.

The dielectric constant rapidly decreases in the low frequency range of 40 Hz to 10 kHz which suggests that strong dielectric relaxation occurs in the samples at low frequencies. The dielectric relaxation originating from the dipole motions or ionic polarization occurs in the frequency range ($f < 10^{10}$ Hz)[55] and is thought to be responsible for the lowering of dielectric constant in the present case. In addition, the dielectric measurements for the dehydrated sample of compound **2** (Fig. S5, ESI) revealed a drastic lowering of the κ value from 5.36 to 3.38 (10 kHz), indicating the removal of highly polar water molecules. Compound **1** belongs to the first generation of dielectric materials (κ = 2.9–3.5)[27] where the dielectric constant drops from 4.76 (40 Hz) to 3.03 (10 kHz). It was also observed that, the dielectric loss (Fig. 4b) remained constant with a value < 0.01 for compound **1** and < 0.2 for compound **2**.

3.4 Impedance Spectroscopy

To further investigate the dielectric behavior of compounds **1** and **2**, impedance spectroscopy studies (Z′ vs Z″) were carried out at room temperature. Complex impedance plots of the two compounds are shown in Fig. 5a. These plots have a semicircular arc in lower resistance region corresponding to bulk material properties and are followed by a spike in the higher resistance region, which corresponds to the formation of electrical double layer capacitances at the electrode/sample interface.[56] As indicated by the plots, the impedance values for compound **1** have a much steeper slope, compared to compound **2**. Impedance vs frequency plots are shown in Fig. 5b. The impedance Z of an ideal capacitor is shown by the formula $Z = 1/j\omega C$, where ω is the angular frequency and C is the electrostatic capacitance of the capacitor. According to the said formula, the amount of impedance decreases inversely with the frequency as shown in Fig. 5b.

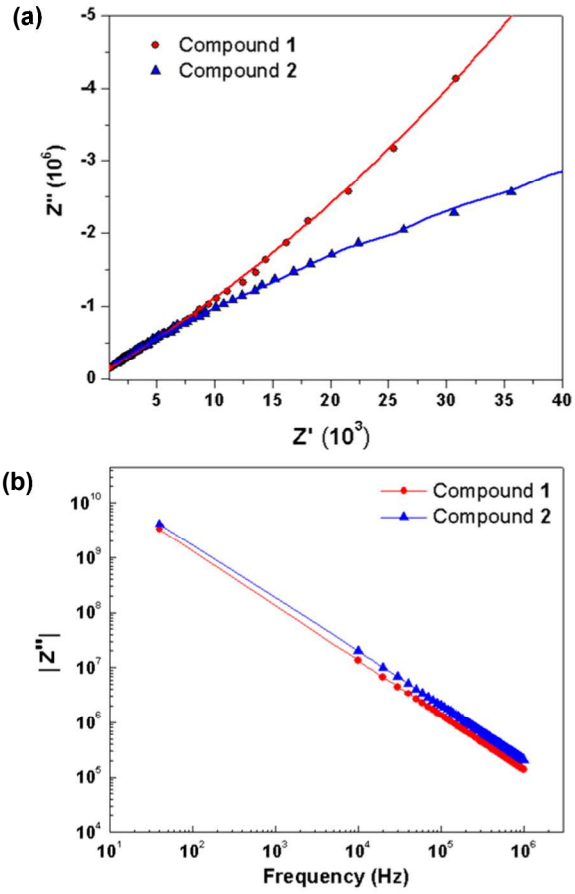

Fig. 5 (a) Impedance plots of compounds **1** and **2**, (b) The corresponding variation of dielectric loss with change in frequency.

4. Conclusion

To summarize, we have investigated the dielectric properties of two thermally stable Ni(II)-based supramolecular networks, which were prepared using a chelating ligand like bisbenzimidazole. The two compounds possess completely different types of polar guest molecules. Dielectric measurements indicate a significant reduction in the value of the dielectric constant ($\varepsilon'_r(\omega)$) when the highly polarizable guest molecules in compound **2** ($\varepsilon'_r(\omega)$ = 12.6 at 40 Hz) were replaced by less polarizable ones in compound **1** ($\varepsilon'_r(\omega)$ = 4.76 at 40 Hz). This decrease can be attributed to the dimerization of acetate counteranions with rare C–H···O hydrogen bonding interactions and localized hydrogen-bonding in compound **1**, while this type of restriction and dimerization is not possible in compound **2**, due to the extensive hydrogen bonding between highly polar guest water molecules, halide ions and the N–H groups of the ligand which creates an electrical order. In addition, in comparison to SiO_2 ($\varepsilon'_r(\omega)$ = 3.91), compound **1** was found to be a good low-κ material ($\varepsilon'_r(\omega)$ = 3.03 at 10 kHz) in the high frequency region. This fundamental study based on structure gives us an insight into the design of both high and low-κ materials with a judicious selection of guest molecules.

Acknowledgements

We thank Academia Sinica and Taiwan International Graduate Program for the financial support. We would like to deeply acknowledge Mr. Ting-Shen Kuo from National Taiwan Normal University for his contribution in solving the crystals.

Notes and references

[a]Institute of Chemistry, Academia Sinica, Taipei 115, Taiwan. Tel: 886-2-27898518; E-mail: kllu@gate.sinica.edu.tw.
[b]Department of Chemistry, National Taiwan University, Taipei 106, Taiwan.
[c]Taiwan International Graduate Program, Nanoscience and Technology Program, Academia Sinica, Taipei 115, Taiwan.
[d]Institute of Physics, Academia Sinica, Taipei 115, Taiwan.

Electronic Supplementary Information (ESI) available: Coordination modes of H_2bbim, FTIR spectra, PXRD patterns, Bond lengths and angles

around Ni(II) in **1** and **2** and crystallographic data. CCDC reference numbers 983051-983052. See DOI: 10.1039/b000000x/

1. N. A. Esipenko, P. Koutnik, T. Minami, L. Mosca, V. M. Lynch, G. V. Zyryanov and P. Anzenbacher, *Chem. Sci.*, 2013, **4**, 3617–3623.
2. Y. Liu, T. Minami, R. Nishiyabu, Z. Wang and P. Anzenbacher, *J. Am. Chem. Soc.*, 2013, **135**, 7705–7712.
3. T. Minami, N. A. Esipenko, B. Zhang, M. E. Kozelkova, L. Isaacs, R. Nishiyabu, Y. Kubo and P. Anzenbacher, *J. Am. Chem. Soc.*, 2012, **134**, 20021–20024.
4. K. Liu, Y. Yao, Y. Kang, Y. Liu, Y. Han, Y. Wang, Z. Li and X. Zhang, *Sci. Rep.*, 2013, **3**, 1–7.
5. J. H. R. Tucker, in *Supramolecular Chemistry*, John Wiley & Sons, Ltd, 2012.
6. A. B. Wolk, E. Garand, I. M. Jones, A. D. Hamilton and M. A. Johnson, *J. Phys. Chem. A*, 2013, **117**, 5962–5969.
7. J. V. Gavette, N. S. Mills, L. N. Zakharov, C. A. Johnson, D. W. Johnson and M. M. Haley, *Angew. Chem. Int. Ed.*, 2013, **52**, 10270–10274.
8. C. Gao, S. Silvi, X. Ma, H. Tian, A. Credi and M. Venturi, *Chem. Eur. J.*, 2012, **18**, 16911–16921.
9. R. Klajn, J. F. Stoddart and B. A. Grzybowski, *Chem. Soc. Rev.*, 2010, **39**, 2203–2237.
10. Z. J. Wang, K. N. Clary, R. G. Bergman, K. N. Raymond and F. D. Toste, *Nat. Chem.*, 2013, **5**, 100–103.
11. J. Meeuwissen and J. N. H. Reek, *Nat. Chem.*, 2010, **2**, 615–621.
12. P. Axe, S. D. Bull, M. G. Davidson, M. D. Jones, D. E. J. E. Robinson, W. L. Mitchell and J. E. Warren, *Dalton Trans.*, 2009, 10169–10171.
13. D. Kaufmann and R. Boese, *Angew. Chem. Int. Ed.*, 1990, **29**, 545–546.
14. F. Herbst, D. Döhler, P. Michael and W. H. Binder, *Macromol. Rapid Commun.*, 2013, **34**, 203–220.
15. L. R. Hart, J. L. Harries, B. W. Greenland, H. M. Colquhoun and W. Hayes, *Polym. Chem.*, 2013, **4**, 4860–4870.
16. T. Aida, E. W. Meijer and S. I. Stupp, *Science*, 2012, **335**, 813–817.
17. M. Burnworth, L. Tang, J. R. Kumpfer, A. J. Duncan, F. L. Beyer, G. L. Fiore, S. J. Rowan and C. Weder, *Nature*, 2011, **472**, 334–337.
18. S. Matile and N. Sakai, in *Analytical Methods in Supramolecular Chemistry*, Wiley-VCH Verlag GmbH & Co. KGaA, 2012, 711–742.
19. T. M. Fyles, *Chem. Soc. Rev.*, 2007, **36**, 335–347.
20. P. Talukdar, G. Bollot, J. Mareda, N. Sakai and S. Matile, *Chem. Eur. J.*, 2005, **11**, 6525–6532.
21. T.-T. Luo, H.-C. Wu, Y.-C. Jao, S.-M. Huang, T.-W. Tseng, Y.-S. Wen, G.-H. Lee, S.-M. Peng, and K.-L. Lu, *Angew. Chem. Int. Ed.*, 2009, **48**, 9461–9464.
22. H. J. Schneider, *Applications of Supramolecular Chemistry for 21st Century Technology*, Taylor & Francis, 2012.
23. A. B. Descalzo, R. Martínez-Máñez, F. Sancenón, K. Hoffmann and K. Rurack, *Angew. Chem. Int. Ed.*, 2006, **45**, 5924–5948.
24. Y.-Z. Tang, X.-F. Huang, Y.-M. Song, P. W. H. Chan and R.-G. Xiong, *Inorg. Chem.*, 2006, **45**, 4868–4870.
25. Z. R. Qu, Q. Ye, H. Zhao, D. W. Fu, H. Y. Ye, R. G. Xiong, T. Akutagawa and T. Nakamura, *Chem. Eur. J.*, 2008, **14**, 3452–3456.
26. T. Hang, D.-W. Fu, Q. Ye, H.-Y. Ye, R.-G. Xiong and S. D. Huang, *Cryst. Growth Des.*, 2009, **9**, 2054–2056.
27. K. Zagorodniy, G. Seifert and H. Hermann, *Appl. Phys. Lett.*, 2010, **97**, 251905.
28. W.-J. Ji, Q.-G. Zhai, S.-N. Li, Y.-C. Jiang and M.-C. Hu, *Chem. Commun.*, 2011, **47**, 3834–3836.
29. P. Yang, X. He, M.-X. Li, Q. Ye, J.-Z. Ge, Z.-X. Wang, S.-R. Zhu, M. Shao and H.-L. Cai, *J. Mater. Chem.*, 2012, **22**, 2398–2400.
30. S. Eslava, L. Zhang, S. Esconjauregui, J. Yang, K. Vanstreels, M. R. Baklanov and E. Saiz, *Chem. Mater.*, 2013, **25**, 27–33.
31. R. J. Cava, *J. Mater. Chem.*, 2001, **11**, 54–62.
32. K. Maex, M. R. Baklanov, D. Shamiryan, F. lacopi, S. H. Brongersma and Z. S. Yanovitskaya, *J. Appl. Phys.*, 2003, **93**, 8793–8841.
33. W. Volksen, R. D. Miller and G. Dubois, *Chem. Rev.*, 2009, **110**, 56–110.
34. B.-H. Yang, H.-Y. Xu, Z.-Y. Yang and C. Zhang, *J. Mater. Chem.*, 2010, **20**, 2469–2473.
35. Y. Zhou, C. Tian, S. Meng, Z. Yue and L. Li, *J. Am. Cer. Soc.*, 2012, **95**, 1665–1670.
36. C.-M. Leu, Y.-T. Chang and K.-H. Wei, *Chem. Mater.*, 2003, **15**, 3721–3727.
37. M. Sánchez-Andújar, S. Yáñez-Vilar, B. Pato-Doldán, C. Gómez-Aguirre, S. Castro-García and M. A. Señarís-Rodríguez, *J. Phys. Chem. C*, 2012, **116**, 13026–13032.
38. D.-W. Fu, J. Dai, J.-Z. Ge, H.-Y. Ye and Z.-R. Qu, *Inorg. Chem. Commun.*, 2010, **13**, 282–285.
39. R.-J. Xu, D.-W. Fu, J. Dai, Y. Zhang, J.-Z. Ge and H.-Y. Ye, *Inorg. Chem. Commun.*, 2011, **14**, 1093–1096.
40. J.-W. Lin, P. Thanasekaran, J.-S. Chang, J.-Y. Wu, L.-L. Lai and K.-L. Lu, *CrystEngComm*, 2013, **15**, 9798–9810.
41. J.-F. Yin, J.-G. Chen, J.-T. Lin, D. Bhattacharya, Y.-C. Hsu, H.-C. Lin, K.-C. Ho and K.-L. Lu, *J. Mater. Chem.*, 2012, **22**, 130–139.
42. J.-Y. Wu, S.-M. Huang, Y.-C. Huang and K.-L. Lu, *CrystEngComm*, 2012, **14**, 1189–1192.
43. P. Thanasekaran, T.-T. Luo, J.-Y. Wu and K.-L. Lu, *Dalton Trans.*, 2012, **41**, 5437–5453.
44. S.-H. Lin, C.-I. Yang, T.-S. Kuo, M.-H. Chiang, K.-C. Hsu and K.-L. Lu, *Dalton Trans.*, 2012, **41**, 1448–1450.
45. C.-I. Yang, P.-H. Chuang and K.-L. Lu, *Chem. Commun.*, 2011, **47**, 4445–4447.
46. P. Thanasekaran, T.-T. Luo, C.-H. Lee and K.-L. Lu, *J. Mater. Chem.*, 2011, **21**, 13140–13149.
47. G. M. Sheldrick, *Acta Crystallogr. A*, 2008, **64**, 112–122.
48. L. Farrugia, *J. Appl. Crystallogr.*, 1999, **32**, 837–838.
49. A. A. Ayi, A. Choudhury, S. Natarajan and C. N. R. Rao, *New J. Chem.*, 2001, **25**, 213–215.
50. Y.-R. Zhong, M.-L. Cao, H.-J. Mo and B.-H. Ye, *Cryst. Growth Des.*, 2008, **8**, 2282–2290.
51. H. Fröhlich, *Theory of dielectrics: dielectric constant and dielectric loss*, Clarendon Press, 1958.
52. C. J. F. Böttcher, O. C. van Belle, P. Bordewijk and A. Rip, *Theory of electric polarization*, Elsevier Scientific Pub. Co., 1978.
53. P. Jain, N. S. Dalal, B. H. Toby, H. W. Kroto and A. K. Cheetham, *J. Am. Chem. Soc.*, 2008, **130**, 10450–10451.
54. P. Jain, V. Ramachandran, R. J. Clark, H. D. Zhou, B. H. Toby, N. S. Dalal, H. W. Kroto and A. K. Cheetham, *J. Am. Chem. Soc.*, 2009, **131**, 13625–13627.
55. Q. Chen, P.-C. Guo, S.-P. Zhao, J.-L. Liu and X.-M. Ren, *CrystEngComm*, 2013, **15**, 1264–1270.
56. S. C. R. J. Sengwa, *Indian J. Pure Appl. Phys.*, 2011, **49**, 204–213.

Table of Contents

Nickel-containing low dielectric and thermally stable supramolecular compounds were synthesized hydrothermally. The frequency dependent dielectric properties of compound **1** were compared with those of compound **2**. Dielectric studies revealed a significant decrease in the value of the dielectric constant when highly polarizable guest molecules in compound **2** ($\varepsilon'_r(\omega)$ = 12.6 at 40 Hz) were replaced by less polarizable ones in **1** ($\varepsilon'_r(\omega)$ = 4.76 at 40 Hz). A single-crystal X-ray diffraction analysis, along with dielectric studies suggests that, the guest molecules play a crucial role in regulating the dielectric constant of this material. This study serves as a motivation to expand our research to create both high and low-κ materials with a judicious selection of guest molecules.